# Stable Nanopores in Two-Dimensional Materials for Ion Conductivity Devices and Biosensors

Hao-Wei Guo[1], Yang-Jun Cui[1], Yu-Zhe Zhang[1], Yun-Long Wang[1], Bao-Wang Su[1], Wen-yuan Zhou[1], Jian-Guo Tian[1,2,3], Cui-Feng Ying[4], Zhi-Bo Liu[1,2,3,*]

[1] The Key Laboratory of Weak Light Nonlinear Photonics, Ministry of Education, School of Physics and Teda Applied Physics Institute, Nankai University, Tianjin 300071, China

[2] Renewable Energy Conversion and Storage Center, Nankai University, Tianjin 300071, China

[3] The collaborative Innovation Center of Extreme Optics, Shanxi University, Taiyuan, Shanxi 030006, China

[4] Advanced Optics & Photonics Laboratory, Department of Engineering, School of Science & Technology, Nottingham Trent University, Nottingham NG11 8NS, UK

ABSTRACT: Highly stable nanopores with precise size and thin thickness are essential to ultrasensitive molecular biosensors and efficient ion filters. However, the stability of both solid-state nanopores and biological nanopores is within a few hours. Even for two-dimensional (2D) materials with excellent properties, it is very difficult to prepare nanopores with stability for more than one day. Here, in mechanical exfoliated 2D materials with excellent quality, highly stable nanopores have been fabricated. Through manual control of defect density and laser spot

irradiation, the breakdown process is more controllable. Nanopore diameter can be precisely adjusted from 1nm to 10nm. The 2 nm-thick graphene nanopore (with a diameter of 2 nm) maintains good consistency in conductivity during the one-month immersion in KCl (1M) solution. The pore size changes less than 0.7% per day. We found that 2D materials nanopores can produce a strong rectification ratio (~50) due to the morphology undulation. In addition, our devices can recognize modified 5nm Au nanoparticles (AuNPs), showing great potential for single-molecule detection. This work can guide the development of high-quality ion rectifier devices and biosensors based on 2D materials nanopores.

TEXT

A nanopore is a kind of single-molecule biosensor based on the Coulter counting principle.[1] The blocked current is generated when the target molecule passes through the pore. It can realize substances detection in a variety of dispersion systems and reflect molecular information such as structure, polarity, and charge of the target molecule.[2] The resolution of a nanopore is directly related to the diameter and length of the ion channel.[3] As a label-free electrical measurement method, nanopores can be divided into biological nanopores and solid-state nanopores according to their materials.[4] In the past few years, high-throughput biosensor devices based on biological nanopores have been extensively researched. Representative α-hemolysin, MspA protein, Aerolysin, and other bio-nanopores have achieved mononuclear DNA detection with multiple-base resolution.[5] Common solid-state nanopores in the insulating membranes (such as silicon nitride, silicon dioxide, and alumina) exhibit better thermal, chemical, and mechanical stability than biological nanopores. It is more conducive to integration into electronic equipment and their pore size are easier to be controlled.[5-7] Unfortunately, the common solid nanopores are still unable

to obtain satisfactory high-quality signals.[8, 9] Most importantly, the stability of the currently prepared nanopores, whether solid-state nanopores or biological nanopores, is within a few hours.[10, 11] Poor stability limits the wide application of nanopores in long-period and complex environments.

Two-dimensional (2D) materials with atomic thickness and excellent mechanical properties[12] provide new options for nanopores. In recent years, the research on 2D materials nanopores represented by graphene[13] and molybdenum disulfide ($MoS_2$)[14, 15] has shown great potential in DNA sequencing and ion filtration. The fabrication methods of 2D materials nanopores include transmission electron microscope (TEM)[16, 17], focused ion beam (FIB)[18], controlled breakdown (CBD)[19, 20], etc. However, compared with the common solid-state nanopores, the 2D materials nanopores do not have obvious advantages in stability, which cannot meet the long-term testing or repeated use. In addition, the high defect density in the 2D materials prepared by the widely used chemical vapor deposition (CVD), exacerbates the instability of the nanopore. Therefore, how to prepare highly stable nanopores in 2D materials while maintaining spatial resolution is the primary challenge of current research.

This article introduces a technical route to fabricate stable nanopores in 2D materials with precise size control. Through manual control of defect density and laser irradiation assisted breakdown, we have successfully fabricated high-quality nanopores in graphene, black phosphorus (BP), molybdenum disulfide ($MoS_2$), and tungsten diselenide ($WSe_2$). The graphene nanopores prepared by this method exhibit good stability and the thickness is precisely controllable (accurate to the atomic level). In addition, we have done research on 2D material nanopores as ion rectifier devices and biosensors. This work can guides the future research of 2D materials nanopores.
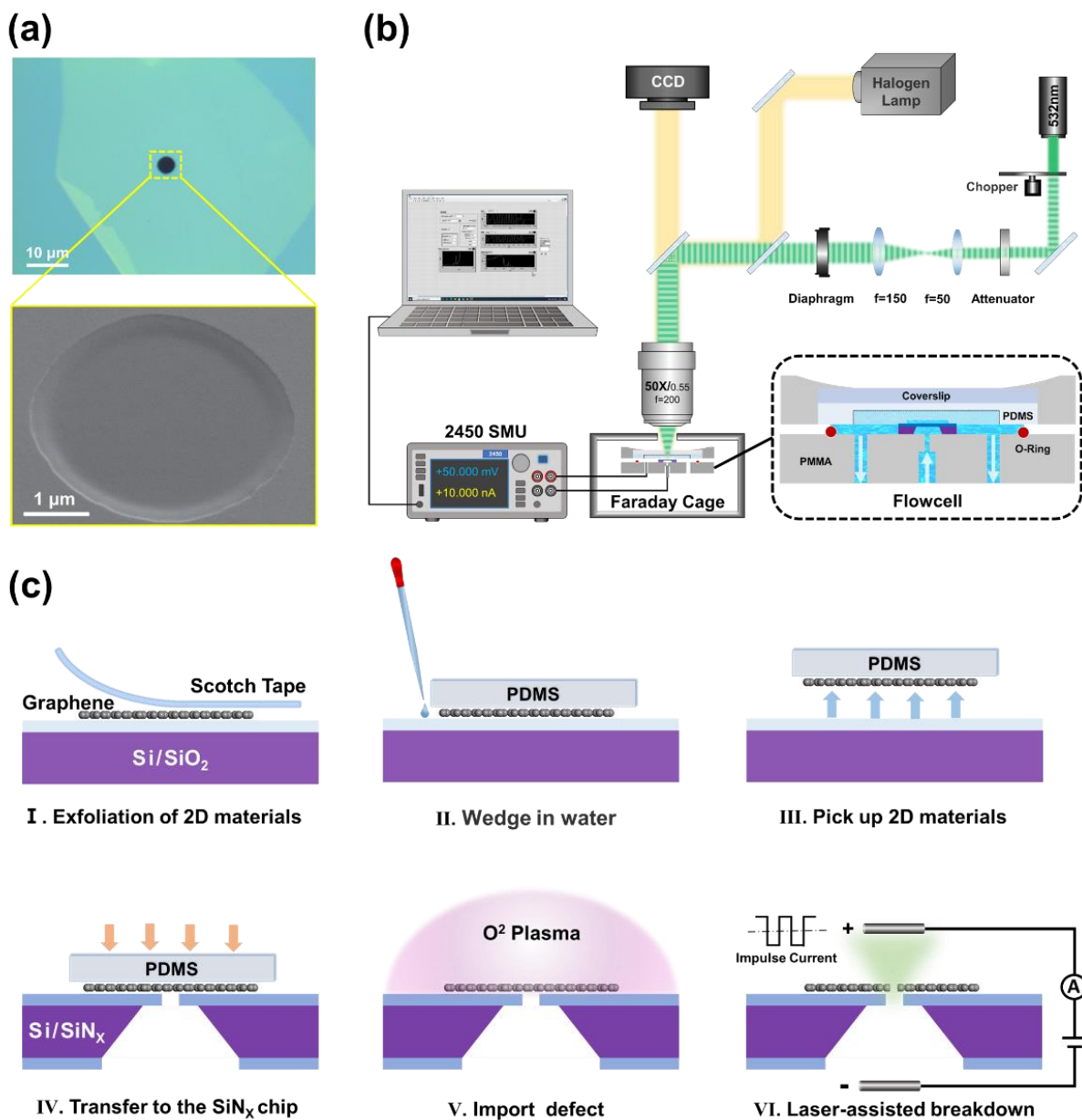
**Figure 1.** Fabrication of nanopores in 2D materials. (a) Microscopic images (top) and scanning electron microscope image (bottom) of MLG sample on a 4 μm nanohole. (b) Schematic drawing of the experimental setup used for nanopore fabrication. The inset provides the schematic of the

flowcell. (c) Nanopore fabrication process. The detailed introduction can be found in the supporting information.

At present, the CBD method has been widely explored in nanopore fabrication for its low-cost equipment and no additional ionization damage on the membrane. However, it is challenging to make nanopores smaller than 10 nm in mechanical exfoliated 2D materials. There are three proposed mechanisms for the formation of nanopores by the CBD method: discharge breakdown, thermal breakdown, and electrochemical breakdown.[21] All mechanisms depend on the generation of defects inside the solid-state film. 2D materials peeled off from natural crystals have extremely high quality.[22] **Figure 1a** shows the suspended structure prepared by mechanical exfoliated graphene. In theory, the nanopore prepared by this structure will have excellent stability. The mechanical exfoliated 2D materials have a stable lattice structure and extremely low defect density. In addition, each layer is independent of each other hence the defects cannot transfer across layers. Therefore, it is difficult to apply a constant voltage to cause effective defect accumulation in the 2D materials. Multiple-layer (i.e. >1L) mechanical exfoliated 2D materials are much more difficult to break down than single-layer 2D materials. In the nanopore fabrication process, the breakdown time is either too long or the initial pore size is too large.

In our research, we significantly increased the success rate of forming nanopores by artificially introducing surface defects through plasma etching, supplemented by laser irradiation[23] (as shown in **Figure 1c**). **Figure 1b** shows the schematic diagram of the equipment used in our experiment. A laser beam (532 nm) irradiates the suspended 2D materials to activate the covalent bond and reduce the breakdown barrier. The laser beam is modulated to 200 Hz, with an average power controlled at 10mW to reduce undesired photochemical reactions. The lowest power that can be ignited (17.1%, rated power 200W) is selected as the etching power. The plasma etching process

can be divided into three stages: the surface coated stage, the surface defect stage, and the deep defect stage. **Figure 2a** shows the TEM images and associated schemes of these three stages, respectively. In the surface coated stage (0 s – 15 s), the defects grow slowly. Plasma etching is mainly used to remove oxygen and water adsorbed on the surface of graphene.[24]Atomic force microscopy images in **Figure 2c** show that the thickness of the film decreases slightly at the surface coated stage, from 1 nm at 0 s to 0.8 nm at 15 s； In the surface defect stage (15 s – 30 s), the plasma etching only destroys the surface lattice structure leading to a rapid increase in the defect density. At this stage, the thickness (0.8 to 0.75 nm) and mechanical strength of the 2D materials films do not decrease significantly. In the deep defect stage (30 s – 60 s), the atoms in the interior layer begin to be affected by plasma etching, and the defect density tends to be saturated. At this stage, we observed a significant decrease in the thickness of the 2D materials (0.75 to 0.3 nm), even the suspended support structure could not be formed. As the number of layers increases, the time for the defect saturation stage appears later shifts. Multi-layer graphene has higher structural stability than single-layer graphene,[25] because of the van der Waals adsorption of interior atoms to the surface-layer atoms. With the homogenization of van der Waals forces between multiple layers, the time to generate defects in 2 to 10 layers graphene is quite close. Raman spectroscopy in **Figure 2c** evaluates the defect type and defect density of 2D materials.[26] The defect density can be characterized by the ratio of Raman peak intensity $I_D/I_G$ (**Figure 2b**).[27] It can be expressed as:

$$L_D^2 = \frac{(4.3\pm1.3)\times10^3}{E_L^4} \left(\frac{I_D}{I_G}\right)^{-1} \tag{1}$$

where $L_D$ is the minimum distance between adjacent point defects, $E_L$ is the average laser power, $I_D$ and $I_G$ are Raman characteristic peak intensities of graphene. Only $L_D$ is much smaller than the size of the self-supporting silicon nitride hole (1μm), can the electrical breakdown process occur.

It is worth noting that we use $I_D/I_G$ to describe the change in the number of defects, which does not reflect the actual value of defect density value. This condition can be met in the entire surface defect stage according to equation (1).
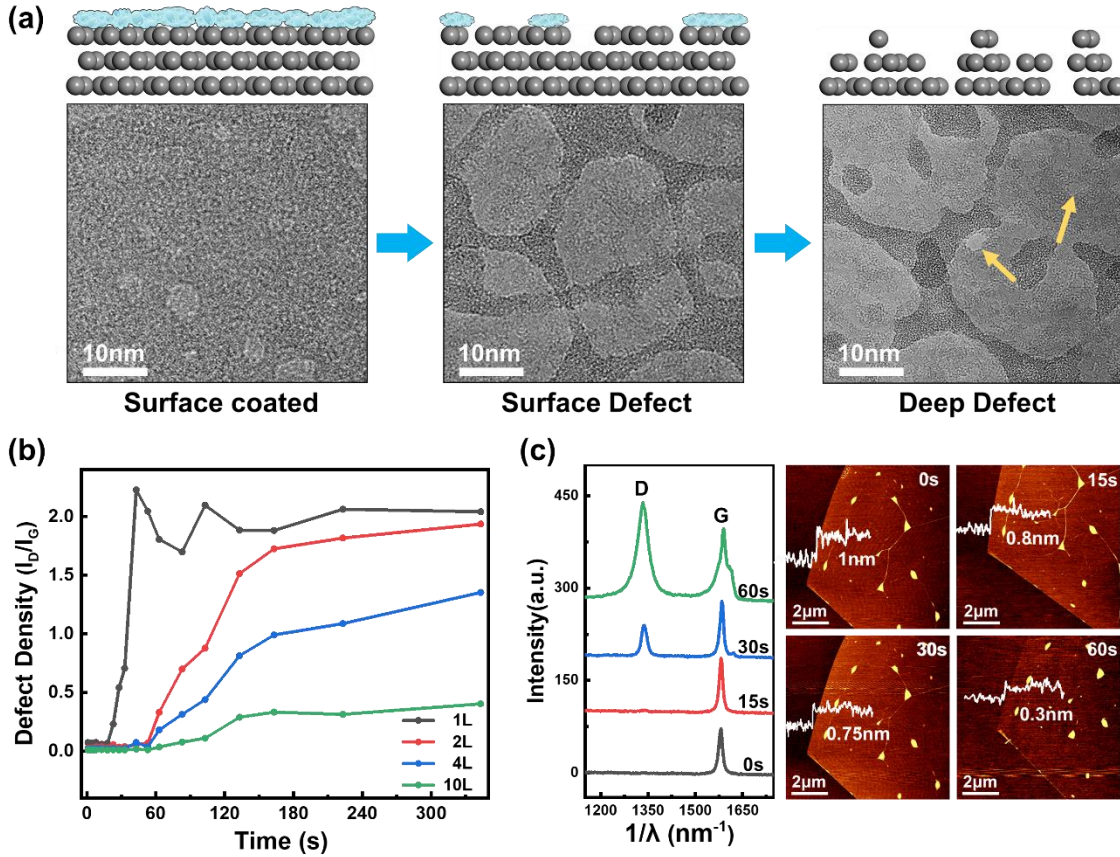


**Figure 2.** graphene plasma etching. (a) Diagrams of graphene lattice structure (top) andand the representative transmission electron microscope (TEM) images (below) for three different stages in the etching process of graphene. (b) The change of graphene defect density over time. Different curves represent different layers of graphene samples. (c) Raman spectroscopy of the bilayer graphene at different etching stages (left), and the corresponding AFM images (right).

There are obvious differences in film thickness and defect density between each sample. Using a fixed voltage (or a fixed electric field strength) cannot guarantee the consistency of the breakdown process. Therefore, a gradually increasing pulse current is used for nanopore fabrication. This pulse current starts at an initial current (10 μA) and gradually increases with an increment of (5 μA). When the source meter (Keithley 2450B) detects that the nanopore size exceeds 1nm, the applied current is rapidly reduced to 1 μA and maintained for 5 minutes to stabilize the nascent pore structure. Similarly, the pore enlargement process still uses a gradually increasing pulse current, and the parameters of the initial current and the current increment are consistent with the breakdown process. The change in nanopore diameter during the complete nanopore fabrication process is shown in **Figure 3a**, for treated and untreated graphene films.
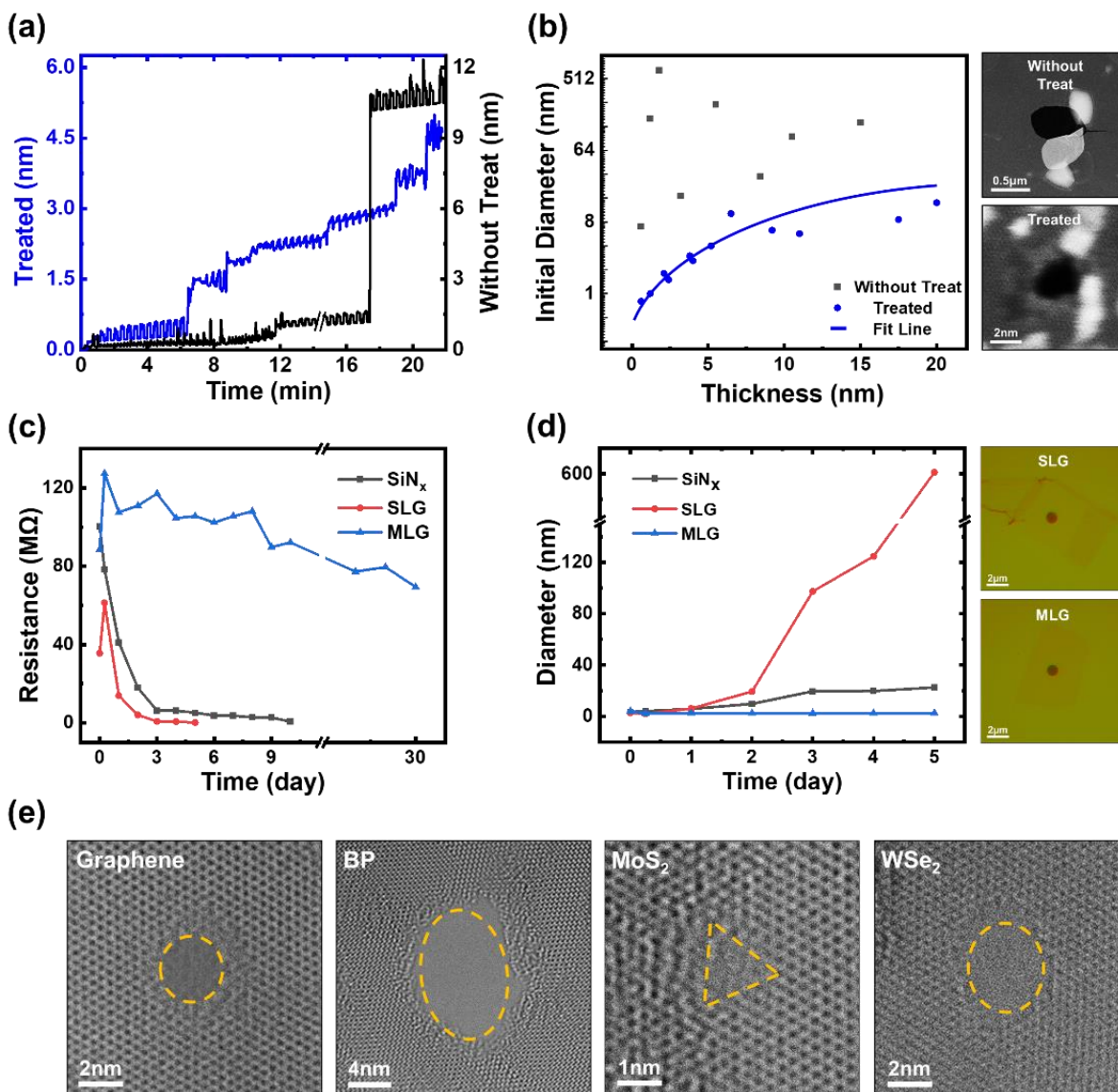
**Figure 3.** Controlled breakdown to fabricate nanopores in 2D materials. (a) Pore diameter changes during the breakdown process and enlargement process for plasma-treated (blue) and untreated (black) graphene films, respectively. The graphene film are 2 nm in thickness for both samples. (b) Initial diameters of breakdown nanopores in graphene films of different thicknesses, with or without plasma treatment. The blue solid curve represents the linear fitting to the initial diameter and film thickness of treated graphene. The TEM images on the right show the representative nanopore images for the untreated (top) and treated (bottom) graphene films.(c,d) Changes of

measured resistance (c) and the diameter (d) of nanopores over days in three different films. The right insets of panel d are microscopy images of SLG and MLG graphene films on a SiN$_x$ hole. © TEM images of nanopores in various 2D materials.

The breakdown process of treated graphene film is easier to precisely control. The initial pore size is much smaller than that of the sample without defect introduction under the same conditions. Most of the treated samples shown in **Figure 3b** have an initial pore size of less than 10nm. The initial pore size and the thickness of the graphene film show a positive correlation, and the breakdown path no longer satisfies the Weibull distribution.[28] In the enlargement process, the size of the graphene nanopores showed a discontinuous, step-wise growth trend. The breakage of the graphene film gradually grows in lattice units, which is consistent with the result of Feng *et al.*[20] Through this method, we have successfully fabricated high-quality nanopores in 2D materials films such as graphene, BP, MoS$_2$, and WSe$_2$ (as shown in **Figure 3e**). The initial shape of these nanopores is related to the selected 2D materials lattice structure. And all samples have a regular vertical profile, which is conducive to reducing the structural differences between each device.

We compared the stability of CBD nanopores with diameters of 2 nm in 10-nm thick SiN$_x$, 2-nm thick multilayer graphene (MLG), and 0.8-nm thick single-layer Graphene (SLG) (**Figures 3c** and **3d**). Previous research reported that the resistance of solid-state nanopores immersed in the electrolyte solution will decrease over time.[29] Three groups of nanopores were immersed in 1M KCl solution (pH = 8.0), and continuously measured at a voltage of 200mV for 1 hour each day to simulate daily use under real conditions. After each test, its pore size was calculated with the average current. The flowcells are replaced with fresh solution before each measurement to eliminate the conductivity deviation caused by the liquid volatilization. SLG nanopore undoubtedly exhibits poor stability and its pore size has grown to more than 100nm in 3 days. On

the contrary, the MLG (2 nm) nanopore exhibits amazing robustness. Even after a one-month immersion test, it still maintained good pore size consistency. The average daily change in pore size is less than 0.7%, which is smaller than the change of nanopores in the thicker $SiN_x$ (10 nm). The stability of nanopores is related to the pore shape and defect density.[29] In the electrolyte solution, the continuous growth of defects causes the size of the nanopores to increase continuously. The layers of the MLG are independent of each other and the defects are difficult to transfer between them. This structural feature effectively prevents the pore size increasing. During the immersion test, the pore size of both two graphene samples decreased significantly in the first few hours. We consider that is due to the edge of the newly formed nanopore are oxidized or recovered[30]. This phenomenon may also be a reason for the stability of graphene nanopores.
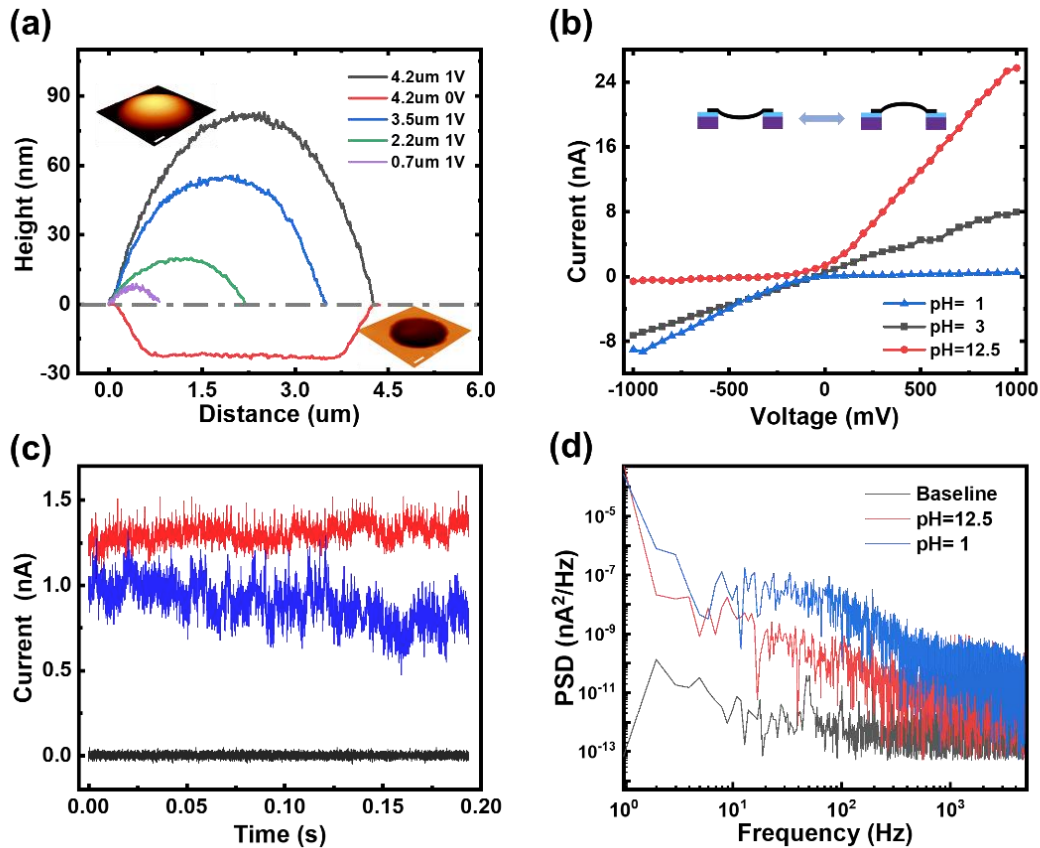
**Figure 4.** Morphology and conductivity of graphene nanopores (a) AFM cross-sections of graphene films with different suspended areas. All the graphene films are about 2 nm thick. The top-left and bottom-right insets are AFM stereograms of 4 µm suspended sample. The scale bar is 1µm. (b) IV curves of a graphene nanopore (5-nm diameter, 2-nm thick) measured in electrolytes buffered at pH 1.0 (blue triangle s), pH 3 (grey squares) and pH 12.5 (red circles). The diameter of the $SiN_x$ hole is about 4 µm. (c) Current traces of the graphene nanopore (used in panel b) at pH 1.0 (blue) and pH 12.5 (red). Data were acquired at 100 mV and digital filtered at 50 kHz. (d) Comparison of the power spectral density (PSD) of the same nanopore in electrolytes buffered at pH 1.0 (blue) and pH 12.5 (red), along with its PSD at 100 mV.

Furthermore, we observed a clear connection between the morphology of 2D materials and the nanopore conductivity (**Figure 4**). This characteristic leads to the amplification of low-frequency noise of graphene nanopores under large suspended areas and in small pH electrolyte solutions (1M KCl).[31] As the area of the suspended 2D materials on the $SiN_x$ hole increases, the morphology undulation affected by external forces also gradually increases. The change of the film morphology can be described by the Hencky model.[32] The cross-section of the 2D materials film is parabolic, which satisfies:

$$H = \delta[1 - (\frac{x-a}{a})^2]\tag{2}$$

where $H$ is the protrusion height of the film, $\delta$ is the deflection of the film, $x$ is the horizontal distance from the edge of the $SiN_x$ hole, and $\alpha$ is the radius of the $SiN_x$ hole. After derivation, it can be obtained that the angle between the film and the $SiN_x$ hole wall satisfies:

$$\theta = atan\left[-2\left(\frac{\Delta f_E a}{K(\vartheta)Et}\right)^{\frac{1}{3}}\right]\tag{3}$$

where $f_E$ is the electric field force, $K(\vartheta)$ is a constant that is dependent on Poisson's ratio $\vartheta$, $E$ is Young's modulus of the film, $t$ is the thickness of the film. When the diameter of the suspended area increases to about 4μm, some nanopores even show obvious ionic current rectification (ICR), as shown in **Figure 4b**. This rectification characteristic is different from the structural rectification produced by asymmetric tapered nanopores[33] or by channels with uneven internal charge distribution.[34] The ICR we observed is induced by the film protrusions or depressions. The modulation of the edge charge density by changing the pH of solutions results in a different electric field force of graphene film. The nanopore device has a higher rectification ratio ($R_r = I_-/I_+$) in an alkaline environment (**Figure 4b**). The finite element simulation (**Figure 5**) confirmed this result, and we get the relationship between nanopore current $I$ and deformation angle $\theta$:

$$I = I_{max} e^{\frac{1}{5}(\frac{\theta - 90}{\theta + 90})} \qquad (4)$$

**Figure 5c** and **Figure 5d** respectively show the change in rectification ratio at different angles and hole positions. By increasing the thickness of the film and reducing the suspended area, the noise level of 2D materials nanopore can be effectively reduced. Conversely, by reducing the thickness of the film and increasing the suspended area, the deformation of the film under the electric field force can be used to prepare fluid valves or ion rectifying devices.
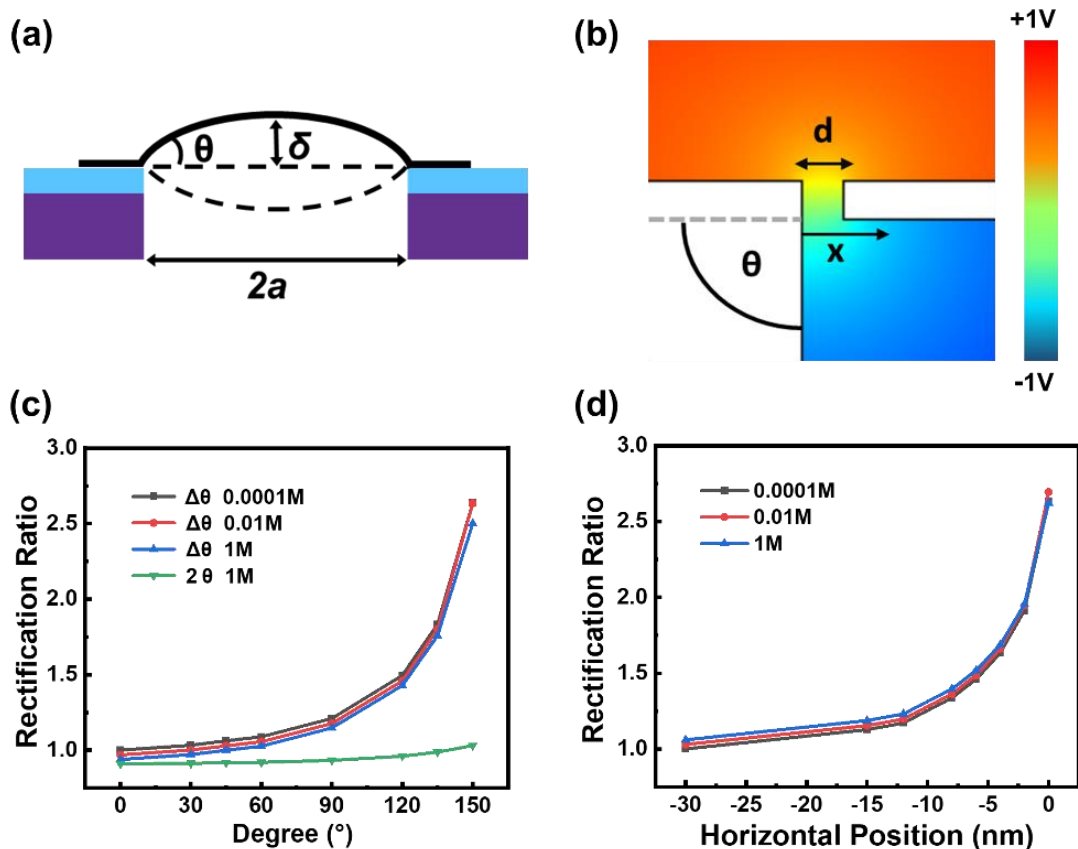
**Figure 5.** Finite-element simulation. (a) Schematic diagram of the cross-section of a nanopore suspended structure. (b) Electric field distribution when a 2D material film is placed perpendicular to the SiN$_x$ hole wall. (c，d) The rectification ratio changes with deformation angle $\theta$ and horizontal distance $x$.

Single-molecule detection is an important application of nanopores. The highly robust 2D material nanopores prepared by our method also have great potential in this field. As a common functional material, Au nanoparticles (AuNPs) can be modified with DNA on the surface. Thus it has specific recognition ability and addressability. We use 5nm AuNPs and the AuNPs modified with 10-base DNA fragments (poly-dG10) as the test substance. Here, our graphene nanopore (2nm thickness, 6.5nm diameter) can clearly distinguish the AuNPs with and without modification. As shown in the Figure 6b, the dewell time of the DNA modified AuNPs was significantly

increased, and the blocked current amplitude was also slightly increased. On individual capture events, the signal of unmodified AuNPs shows a symmetrical sharp peak (Figure 6a right top). The signal of AuNPs after DNA modification is still sharp in the first half, but it becomes smooth in the second half (Figure 6a right bottom). It can be seen that the DNA on the surface of AuNPs can effectively delay the time of it passing through the nanopores.
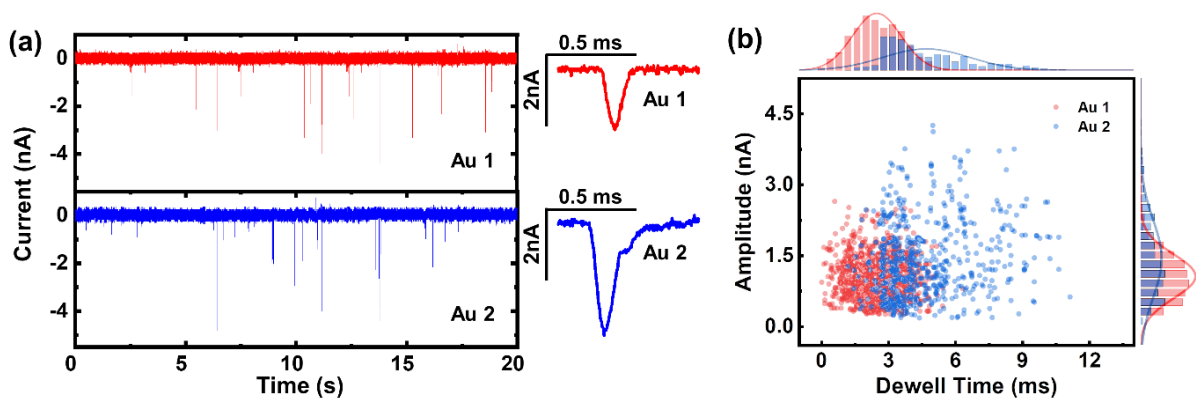


**Figure 6.** Detection of 5nm AuNPs. (a) Signals of AuNPs passing through the graphene nanopores. Au1 (red line) is unmodified AuNPs, Au2 (blue line) is modified AuNPs. (b) Statistical distribution of AuNPs capture events.

In this work, highly stable nanopores in various 2D materials such as graphene, BP, $MoS_2$, and $WSe_2$ have been fabricated. By artificially introducing quantitative defects and laser irradiation, we can easily create high-quality nanopores in mechanical exfoliated 2D materials with thicknesses ranging from 0.5 nm to 20 nm. In addition, the manufacturing precision in pore size can reach 1 nm or less. We found that the initial pore size and the step-growth of nanopores are related to the lattice structure of the 2D materials. The 2-nm MLG nanopores exhibit good stability when immersed in the electrolyte solution. The daily increase in pore size is less than 0.7%. In addition, we have investigated the influence of the suspended 2D material morphology on the

nanopore conductivity. Thin film and large suspended area caused the amplification of low-frequency noise (10-1000 Hz) and deformation rectification. Finally, we successfully detected the DNA-modified AuNPs using the prepared graphene nanopores. This research may promote the research process of 2D material nanopore ion conductivity devices and biosensors.

**TOC**
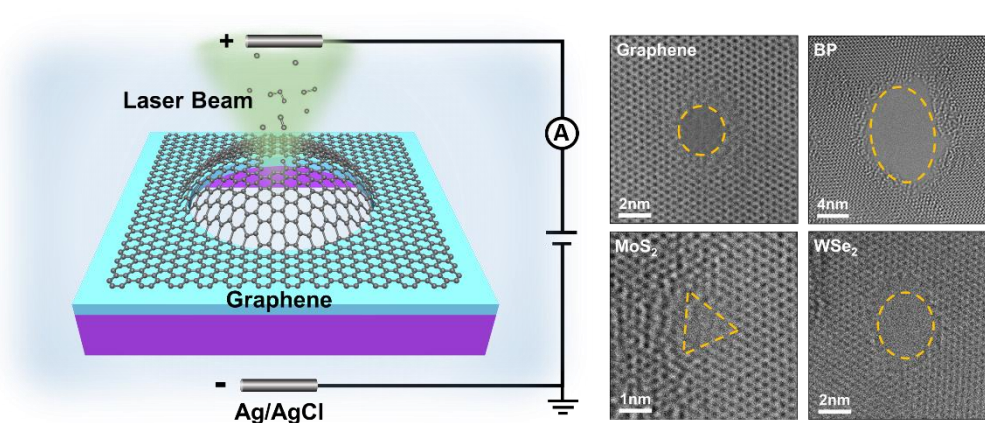


ASSOCIATED CONTENT

 **Supporting Information**. Materials and methods, supplementary Figures.

AUTHOR INFORMATION

**Corresponding Author**

Zhi-Bo Liu - *The Key Laboratory of Weak Light Nonlinear Photonics, Ministry of Education, School of Physics and Teda Applied Physics Institute, Nankai University, Tianjin 300071, China; Renewable Energy Conversion and Storage Center, Nankai University, Tianjin 300071, China; The collaborative Innovation Center of Extreme Optics, Shanxi University, Taiyuan, Shanxi 030006, China; Email:liuzb@nankai.edu.cn*

## Authors

Hao-Wei Guo - *The Key Laboratory of Weak Light Nonlinear Photonics, Ministry of Education, School of Physics and Teda Applied Physics Institute, Nankai University, Tianjin 300071, China*

Yang-Jun Cui - *The Key Laboratory of Weak Light Nonlinear Photonics, Ministry of Education, School of Physics and Teda Applied Physics Institute, Nankai University, Tianjin 300071, China*

Yu-Zhe Zhang - *The Key Laboratory of Weak Light Nonlinear Photonics, Ministry of Education, School of Physics and Teda Applied Physics Institute, Nankai University, Tianjin 300071, China*

Yun-Long Wang - *The Key Laboratory of Weak Light Nonlinear Photonics, Ministry of Education, School of Physics and Teda Applied Physics Institute, Nankai University, Tianjin 300071, China*

Bao-Wang Su - *The Key Laboratory of Weak Light Nonlinear Photonics, Ministry of Education, School of Physics and Teda Applied Physics Institute, Nankai University, Tianjin 300071, China*

Wen-Yuan Zhou - *The Key Laboratory of Weak Light Nonlinear Photonics, Ministry of Education, School of Physics and Teda Applied Physics Institute, Nankai University, Tianjin 300071, China*

Jian-Guo Tian - *The Key Laboratory of Weak Light Nonlinear Photonics, Ministry of Education, School of Physics and Teda Applied Physics Institute, Nankai University, Tianjin 300071, China; Renewable Energy Conversion and Storage Center, Nankai University, Tianjin 300071, China; The collaborative Innovation Center of Extreme Optics, Shanxi University, Taiyuan, Shanxi 030006, China*

Cui-Feng Ying - *Advanced Optics & Photonics Laboratory, Department of Engineering, School of Science & Technology, Nottingham Trent University, Nottingham NG11 8NS, UK*

## Author contributions

G. H. W. and Z. B. L. planned and conducted the experiments and wrote the paper. Y.J.C. assisted in the theoretical analysis of deformation model. H. W. G. and Y. Z. Z. performed the fabrication and characterization of 2DM nanopore. Y.L.W. and C.F.Y assisted in the equipment construction. B. W. S. assisted in the transfer of 2D materials. Z. B. L. and W. Y. Z. developed the ideas and concepts presented here. J. G. T. supervised and directed the research.

Notes

REFERENCES

1.      Coulter, W. H., Means for counting particles suspended in a fluid. US2656508 A[P] **1953**.

2.      Waugh, M.; Briggs, K.; Gunn, D.; Gibeault, M.; King, S.; Ingram, Q.; Jimenez, A. M.; Berryman, S.; Lomovtsev, D.; Andrzejewski, L.; Tabard-Cossa, V., Solid-state nanopore fabrication by automated controlled breakdown. *Nat Protoc* **2020,** *15* (1), 122-143.

3.      Kwok, H.; Briggs, K.; Tabard-Cossa, V., Nanopore Fabrication by Controlled Dielectric Breakdown. *Plos One* **2014,** *9* (3), e92880.

4.      Arcadia, C. E.; Reyes, C. C.; Rosenstein, J. K., In Situ Nanopore Fabrication and Single-Molecule Sensing with Microscale Liquid Contacts. *Acs Nano* **2017,** *11* (5), 4907-4915.

5.      Lee, K.; Park, K. B.; Kim, H. J.; Yu, J. S.; Chae, H.; Kim, H. M.; Kim, K. B., Recent Progress in Solid-State Nanopores. *Adv Mater* **2018,** *30* (42), e1704680.

6.      Perez-Mitta, G.; Toimil-Molares, M. E.; Trautmann, C.; Marmisolle, W. A.; Azzaroni, O., Molecular Design of Solid-State Nanopores: Fundamental Concepts and Applications. *Adv Mater* **2019,** *31* (37).

7.      Venkatesan, B. M.; Bashir, R., Nanopore sensors for nucleic acid analysis. *Nat Nanotechnol* **2011,** *6* (10), 615-624.

8.      Branton, D.; Deamer, D. W.; Marziali, A.; Bayley, H.; Benner, S. A.; Butler, T.; Di Ventra,

M.; Garaj, S.; Hibbs, A.; Huang, X.; Jovanovich, S. B.; Krstic, P. S.; Lindsay, S.; Ling, X. S.; Mastrangelo, C. H.; Meller, A.; Oliver, J. S.; Pershin, Y. V.; Ramsey, J. M.; Riehn, R.; Soni, G. V.; Tabard-Cossa, V.; Wanunu, M.; Wiggin, M.; Schloss, J. A., The potential and challenges of nanopore sequencing. *Nat. Biotechnol.* **2008,** *26* (10), 1146-1153.

9.      Park, H. J.; Ryu, G. H.; Zonghoon, L., Hole Defects on Two-Dimensional Materials Formed by Electron Beam Irradiation: Toward Nanopore Devices. *Appl. Microsc.* **2015,** *45* (3), 107-114.

10.     Chou, Y. C.; Das, P. M.; Monos, D. S.; Drndic, M., Lifetime and Stability of Silicon Nitride Nanopores and Nanopore Arrays for Ionic Measurements. *Acs Nano* **2020,** *14* (6), 6715-6728.

11.     Hu, R.; Tong, X.; Zhao, Q., Four Aspects about Solid-State Nanopores for Protein Sensing: Fabrication, Sensitivity, Selectivity, and Durability. *Adv. Healthcare. Mater.* **2020,** *9* (17), 2000933.

12.     Chang, C.; Chen, W.; Chen, Y.; Chen, Y.; Chen, Y.; Ding, F.; Fan, C.; Jin Fan, H.; Fan, Z.; Gong, C.; Gong, Y.; He, Q.; Hong, X.; Hu, S.; Hu, W.; Huang, W.; Huang, Y.; Ji, W.; Li, D.; Li, L.; Li, Q.; Lin, L.; Ling, C.; Liu, M.; Liu, N.; Liu, Z.; Ping Loh, K.; Ma, J.; Miao, F.; Peng, H.; Shao, M.; Song, L.; Su, S.; Sun, S.; Tan, C.; Tang, Z.; Wang, D.; Wang, H.; Wang, J.; Wang, X.; Wang, X.; T. S. Wee, A.; Wei, Z.; Wu, Y.; Wu, Z.; Xiong, J.; Xiong, Q.; Xu, W.; Yin, P.; Zeng, H.; Zeng, Z.; Zhai, T.; Zhang, H.; Zhang, H.; Zhang, Q.; Zhang, T.; Zhang, X.; Zhao, L.; Zhao, M.; Zhao, W.; Zhao, Y.; Zhou, K.; Zhou, X.; Zhou, Y.; Zhu, H.; Zhang, H.; Liu, Z., Recent Progress on Two-Dimensional Materials. *Acta Phys. Chim. Sin.* **2021,** 37 (12), 2108017.

13.     Heerema, S. J.; Dekker, C., Graphene nanodevices for DNA sequencing. *Nat. Nanotechnol.* **2016,** *11* (2), 127-136.

14.     Thakur, M.; Macha, M.; Chernev, A.; Graf, M.; Lihter, M.; Deen, J.; Tripathi, M.; Kis, A.; Radenovic, A., Wafer-Scale Fabrication of Nanopore Devices for Single-Molecule DNA

Biosensing using MoS$_2$. *Small Methods* **2020,** *4* (11), 2000072.

15.     Feng, J.; Liu, K.; Graf, M.; Dumcenco, D.; Kis, A.; Di Ventra, M.; Radenovic, A., Observation of ionic Coulomb blockade in nanopores. *Nat. Mater.* **2016,** *15* (8), 850- 855.

16.     Schneider, G. F.; Kowalczyk, S. W.; Calado, V. E.; Pandraud, G.; Zandbergen, H. W.; Vandersypen, L. M. K.; Dekker, C., DNA Translocation through Graphene Nanopores. *Nano Lett.* **2010,** *10* (8), 3163-3167.

17.     Fischbein, M. D.; Drndic, M., Electron beam nanosculpting of suspended graphene sheets. *Appl. Phys. Lett.* **2008,** *93* (11), 113107.

18.     Deng, Y.; Huang, Q.; Zhao, Y.; Zhou, D.; Ying, C.; Wang, D., Precise fabrication of a 5 nm graphene nanopore with a helium ion microscope for biomolecule detection. *Nanotechnology* **2017,** *28* (4), 045302.

19.     Kuan, A. T.; Lu, B.; Xie, P.; Szalay, T.; Golovchenko, J. A., Electrical pulse fabrication of graphene nanopores in electrolyte solution. *Appl Phys Lett* **2015,** *106* (20), 203109.

20.     Feng, J.; Liu, K.; Graf, M.; Lihter, M.; Bulushev, R. D.; Dumcenco, D.; Alexander, D. T.; Krasnozhon, D.; Vuletic, T.; Kis, A.; Radenovic, A., Electrochemical Reaction in Single Layer MoS2: Nanopores Opened Atom by Atom. *Nano Lett* **2015,** *15* (5), 3431-3438.

21.     Xue, L.; Yamazaki, H.; Ren, R.; Wanunu, M.; Ivanov, A. P.; Edel, J. B., Solid-state nanopore sensors (vol 5, pg 931, 2020). *Nature Reviews Materials* **2020,** *5* (12), 952-952.

22.     Guo, H.; Hu, Z.; Liu, Z.; Tian, J., Stacking of 2D Materials. *Advanced Functional Materials* **2021,** *31* (4), 2007810.

23.     Ying, C.; Houghtaling, J.; Eggenberger, O. M.; Guha, A.; Nirrnalraj, P.; Awasthi, S.; Tian, J.; Mayer, M., Formation of Single Nanopores with Diameters of 20-50 nm in Silicon Nitride Membranes Using Laser-Assisted Controlled Breakdown. *Acs Nano* **2018,** *12* (11), 11458-11470.

24.     Tung, V. C.; Allen, M. J.; Yang, Y.; Kaner, R. B., High-throughput solution processing of large-scale graphene. *Nature Nanotechnology* **2009,** *4* (1), 25-29.

25.     Ryu, S.; Han, M. Y.; Maultzsch, J.; Heinz, T. F.; Kim, P.; Steigerwald, M. L.; Brus, L. E., Reversible Basal Plane Hydrogenation of Graphene. *Nano Letters* **2008,** *8* (12), 4597-4602.

26.     Eckmann, A.; Felten, A.; Mishchenko, A.; Britnell, L.; Krupke, R.; Novoselov, K. S.; Casiraghi, C., Probing the Nature of Defects in Graphene by Raman Spectroscopy. *Nano Letters* **2012,** *12* (8), 3925-3930.

27.     Li, B.; Zhou, L.; Wu, D.; Peng, H.; Yan, K.; Zhou, Y.; Liu, Z., Photochemical Chlorination of Graphene. *Acs Nano* **2011,** *5* (7), 5957-5961.

28.     Briggs, K.; Charron, M.; Kwok, H.; Le, T.; Chahal, S.; Bustamante, J.; Waugh, M.; Tabard-Cossa, V., Kinetics of nanopore fabrication during controlled breakdown of dielectric membranes in solution. *Nanotechnology* **2015,** *26* (8), 084004.

29.     van den Hout, M.; Hall, A. R.;  Wu, M. Y.; Zandbergen, H. W.; Dekker, C.; Dekker, N. H., Controlling nanopore size, shape and stability. *Nanotechnology* **2010,** *21* (11), 115304.

30.     Lee, J.; Yang, Z.; Zhou, W.; Pennycook, S. J.; Pantelides, S. T.; Chisholm, M. F., Stabilization of graphene nanopore. *Proceedings of the National Academy of Sciences of the United States of America* **2014,** *111* (21), 7522-7526.

31.     Heerema, S. J.; Schneider, G. F.; Rozemuller, M.; Vicarelli, L.; Zandbergen, H. W.; Dekker, C., 1/f noise in graphene nanopores. *Nanotechnology* **2015,** *26* (7), 074001.

32.     Wang, L.; Travis, J. J.; Cavanagh, A. S.; Liu, X.; Koenig, S. P.; Huang, P. Y.; George, S. M.; Bunch, J. S., Ultrathin Oxide Films by Atomic Layer Deposition on Graphene. *Nano Letters* **2012,** *12* (7), 3706-3710.

33.     Ali, M.; Ramirez, P.; Mafe, S.; Neumann, R.; Ensinger, W., A pH-Tunable Nanofluidic

Diode with a Broad Range of Rectifying Properties. *Acs Nano* **2009,** *3* (3), 603-608.

34.     Daiguji, H.; Oka, Y.; Shirono, K., Nanofluidic diode and bipolar transistor. *Nano Letters* **2005,** *5* (11), 2274-2280.